Spontaneous self-assembly of thermo-responsive vesicles using a zwitterionic and an anionic surfactant

Thomas M. McCoy,[†,‡] Joshua B. Marlow,[‡] Alexander J. Armstrong,[†] Andrew J. Clulow,[¶] Christopher J. Garvey,[§,‖,⊥] Madhura Manohar,[#] Tamim A. Darwish,[#] Ben J. Boyd,[¶,@] Alexander F. Routh,[*,†] and Rico F. Tabor[*,‡]

†*BP Institute and Department of Chemical Engineering and Biotechnology, University of Cambridge, CB3 0EZ, United Kingdom*

‡*School of Chemistry, Monash University, Clayton 3800, Australia*

¶*Drug Delivery, Disposition and Dynamics, Monash Institute of Pharmaceutical Sciences, Parkville 3052, Australia*

§*Australian Centre for Neutron Scattering, ANSTO, Lucas Heights, New South Wales 2234, Australia*

‖*Biofilm Research Center for Biointerfaces and Biomedical Science Department, Faculty of Health and Society, Malmö University, Malmö, Sweden*

⊥*Lund Institute for Advanced Neutron and X-ray Scattering, Lund, Sweden*

#*National Deuteration Facility, ANSTO, Lucas Heights, New South Wales 2234, Australia*

@*ARC Centre of Excellence in Convergent Bio-Nano Science and Technology, Monash Institute of Pharmaceutical Sciences, Parkville, VIC, 3052, Australia*

E-mail: afr10@cam.ac.uk; rico.tabor@monash.edu

Phone: +61 3 9905 4558. Fax: +61 3 9905 4597

Abstract

Spontaneous formation of vesicles from the self-assembly of two specific surfactants - one zwitterionic (oleyl amidopropyl betaine, OAPB) and the other anionic (Aerosol-OT, AOT) - is explored in water using small-angle scattering techniques. Two factors were found to be critical in the formation of vesicles: surfactant ratio, as AOT concentrations less than equimolar with OAPB result in cylindrical micelles or mixtures of micellar structures, and salt concentration, whereby increasing the amount of NaCl promotes vesicle formation by reducing head-group repulsions. Small-angle neutron scattering measurements reveal that the vesicles are approximately 30-40 nm in diameter depending on sample composition. Small-angle X-ray scattering measurements suggest preferential partitioning of OAPB molecules on the vesicle inner layer to support vesicular packing. Heating the vesicles to physiological temperature (37°C) causes them to collapse into smaller ellipsoidal micelles (2-3 nm), with higher salt concentrations ($\geq$10 mM) inhibiting this transition. These aggregates could serve as responsive carriers for loading or unloading of aqueous cargoes such as drugs and pharmaceuticals, with temperature changes serving as a simple release/uptake mechanism.

Keywords

Self-assembly, vesicles, surfactants, salt, temperature, small-angle scattering.

Introduction

Vesicles are a critical class of molecular self-assembly that take the form of a spherical bilayer.[1,2] Their characteristic core−shell structure forms the foundation of cell biology as lipid membranes, and in industry as capsules or vessels for microreactions[3–5] and drug delivery.[6,7] Despite their ubiquity in nature, spontaneous formation of vesicles in simple laboratory formulations is significantly less common, with many reported systems exhibiting metastability and limited control over size.[8–10] Therefore, uncovering new systems that

spontaneously form vesicles is required to facilitate their implementation in industry and medicine as viable delivery vessels.

Surfactant self-assembly of this nature relies on a specific interplay of thermodynamics, interaction energies and molecular geometry.[2,11] In order for sufficient spontaneous curvature to enable a vesicle to exist, asymmetry between surfactant head and tail-groups must be present so that aggregation does not proceed along a planar axis (lamellae). In turn, this asymmetry must not be so profound that the micelle conforms to higher curvature shapes such as rods and spheres. Surfactant mixtures (two or more) are thus more likely to satisfy these conditions, as different surfactant partitioning between the inner and outer monolayers of the vesicle will yield different spontaneous curvatures.[12] The prevailing shape is then determined by the surfactant ratio, and if the two curvatures are complementary, a curved bilayer (vesicle) will be energetically favoured over a planar bilayer.[13] Choice of surfactants is therefore key in underpinning vesicle formation.

Betaine surfactants are heavily utilised in industry for cosmetic and household products due to their low toxicity[14,15] and minimal capacity for skin irritation.[16,17] In addition, they have the attractive property of spontaneously forming wormlike micelles in solution.[18,19] Wormlike aggregation, like polymers, tends to yield high viscosity fluids due to formation of an entangled molecular network that can store energy elastically.[20–22] However, unlike polymers, wormlike micelles are able to break apart and reform, providing means for controlling fluid properties and earning them the title: 'living polymers'. A vesicle system generated from betaine-based surfactants is desirable as it would possess the benefits of being both low toxicity and dynamic (reversibly assembled and stimuli-responsive).

Previously we have shown formation of anomalously small vesicles (16 nm) from specific mixtures of Aerosol-OT (AOT) and erucyl amidopropyl betaine, attributed to favourable

packing based on surfactant geometry.[23] The present work explores more rigorously the factors driving vesicle self-assembly in a similar system comprising AOT and oleyl amidopropyl betaine, which is cheaper and more commonly used in industry than its erucyl counterpart. Small-angle neutron and X-ray scattering are used to gain structural information whilst the effects of surfactant ratio, salt concentration and temperature are examined to probe physical phenomena and mechanisms for disassembly.

Experimental section

Materials

Oleyl amidopropyl betaine (OAPB, Fig. 1b) was synthesised, purified and desalted as described previously,[24] with the final molecule having a molecular weight of 424.66 g/mol. Sodium bis(2-ethylhexyl) sulfosuccinate (Aerosol-OT, Fig. 1b) was obtained from ChemSupply, Australia ($\geq$90%) and desalted by centrifugation in anhydrous methanol before use. Deuterium oxide (D_2O, 99.8% atom D) was obtained from Merck (Darmstadt, Germany) and used as received. Sodium chloride, potassium chloride, rubidium chloride and cesium chloride (all (>99%) were also obtained from Merck and used as received.

Methods

Small-angle neutron scattering (SANS) measurements were conducted on the QUOKKA beamline[25] at the Australian Centre for Neutron Scattering, ANSTO. Samples were prepared several days in advance by dissolving precise quantities of surfactant in D_2O with stirring. Measurements were performed at either 25 or 37°C in 2 mm path-length, quartz Hellma cells. Raw scattering counts from the detector were reduced to radially averaged absolute intensity profiles ($I(q)$ vs q), normalising against a blocked beam and transmission measurement, and

presented as a function of the scattering vector, q:

$$q = \frac{4\pi}{\lambda} \sin \frac{\theta}{2}$$

where θ is the scattering angle and λ is the wavelength of the incident neutrons (5 Å). Scattering was performed with the detector positioned separately at 2 and then 14 m from the sample environment, providing a q-range of approximately 0.005–0.4 $Å^{-1}$. Absolute intensities were scaled according to the sample thicknesses (2 mm) and using an empty beam measurement. Datasets corresponding to each detector position were manually stitched together using the IGOR Pro macros developed by Kline.[26] Lastly, scattering from an empty cell was subtracted from all final data sets before modelling.

Small-angle X-ray scattering (SAXS) measurements were conducted on the SAXS/WAXS beamline at the Australian Synchrotron, ANSTO.[27] An autoloader sample environment injected each sample into a 1.5 mm quartz capillary. Measurements were performed at 25°C, with consecutive sample–detector distances of 0.96 m and 7.16 m (q-range approximately 0.0025–0.9 $Å^{-1}$) and an X-ray wavelength of 1.033 Å (photon energy = 12 keV). 2D scattering images were collected on a Pilatus 1M detector, and absolute intensity profiles were reduced from the raw counts using the custom software ScatterBrain and water in the quartz capillary as a standard. For SAXS, samples were prepared in a similar fashion using H_2O as the solvent.

Modelling of all scattering data was performed using the software SASView (http://www.sasview.org), version 4.2.0. For all presented data, symbols represent the experimental scattering data and black dashed/dotted lines are the model fits (described throughout). Details of each model are provided in the Supporting Information, as well as tables containing all fitting parameters for producing model fits.

Results and discussion

Oleyl amidopropyl betaine (OAPB) has a zwitterionic headgroup and a 18-carbon singly *cis* unsaturated tail (Fig. 1b). In the absence of AOT, small-angle neutron scattering (SANS) of 10 mM OAPB reveals wormlike aggregation[28,29] (Fig. 1a) with a cross-sectional radius of 2.2 nm (see SI, Fig. S3 and Table S3), consistent with previous findings.[24,30,31] Formation of wormlike micelles for this surfactant stems from the zwitterionic headgroup serving to self-screen intermolecular repulsions, allowing denser packing.[18] The system thus behaves similarly to ionic surfactants with added electrolyte which can aggregate in a similar manner.[32,33] Alternatively, Aerosol-OT (AOT) has an anionic head group and two ethyl-branched 6-carbon tails (Fig. 1b). AOT is found to form charged prolate ellipsoids[34–39] in aqueous solution (Fig. 1a) of radii 1.8 and 1.4 nm (see SI, Fig. S1 and Table S1), which concurs with previous studies.[40–42]

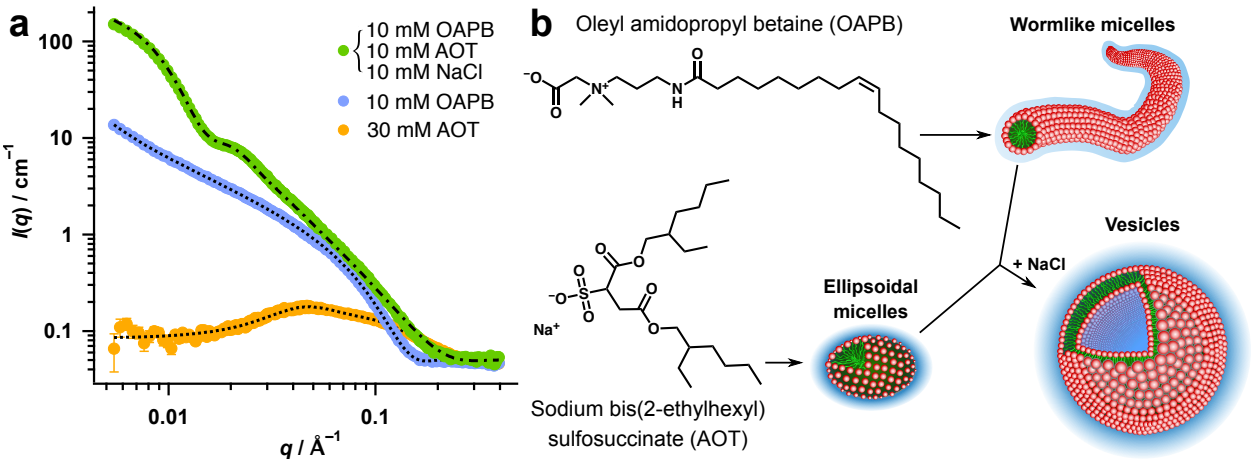

Figure 1: (a) SANS data and model fits of pure OAPB and AOT surfactant solutions (10 mM and 30 mM respectively) and a mixed solution (10 mM OAPB/AOT) with 10 mM NaCl at 25°C. (b) Schematic showing the chemical structures of OAPB and AOT, and their micellar structures when separate (ellipsoids and worms) and when mixed together in the presence of NaCl (vesicles).

When mixed in a minimum ratio of 1:1 (10 mM OAPB:10 mM AOT) with a small addition (10 mmol L^{-1}) of NaCl, these surfactants exhibit the form factor of unilamellar vesicles[43]

(Fig. 1a). For this composition, the vesicles have a core diameter of approximately 31 nm and a shell thickness of 2.1 nm (See SI, Table S4), indicating a mixture of small vesicles with a high spontaneous curvature.[9,11] Notably, the lengths of C18 and C6 hydrocarbon chains are approximately 2.4 and 0.9 nm respectively, according to the Tanford equation.[44] Hence, a shell thickness of 2.1 nm suggests substantial interpenetration between tail-groups of the inner and outer surfactant layers. Additional discrepancy in length can be accounted for by *cis*-unsaturation in the OAPB tail-group causing it to 'kink' (not extend fully) (Fig. 1b), as well as solvation of head-groups serving to mask their scattering signature.

When combined, OAPB and AOT act synergistically to self-assemble into vesicles (Fig. 1b). These molecules are not dissimilar to biological phospholipids which also typically have either zwitterionic or anionic head-groups and long unsaturated tails; these features allow such molecules to naturally pack into bilayers.[1] For OAPB and AOT, it is likely that charge-based attraction occurs between the quaternary ammonium group in OAPB and the AOT sulfonate group, allowing denser molecular packing and thus lower curvature interfaces than the pure surfactant solutions. As such this system can be considered similar to the ubiquitous vesicle systems formed from mixtures of cationic and anionic surfactants.[13,45,46]

However, the inclusion of salt appears to be a critical factor in driving vesicle self-assembly in this system (Fig. 2a). When observing SANS from a solution of 10 mM OAPB and 20 mM AOT without any additional salt, a mixture of vesicles and predominantly charged ellipsoids is present. When salt is incrementally added, the 'bulge' at medium q becomes progressively less pronounced, which corresponds to fewer ellipsoidal or cylindrical micelles being present (inset of Fig. 2a). At 10 mM NaCl, the system consists purely of unilamellar vesicles with a volume fraction of 1.27% compared to 0.08% at 0 mM NaCl (Fig. 2a). This equates to an approximately 16-fold increase in the number of vesicles. Further additions of NaCl up to 50 mM cause little subsequent change in aggregation, with vesicle volume fraction increasing

only a small amount to 1.35% and total vesicle diameter consistent at around 40 nm (see SI, Table S5), indicating that a limiting spontaneous curvature has been reached.

Similar to the previously described head-group interactions, addition of salt is likely to cause further charge screening that serves to promote a lower curvature equilibrium geometry. This added shielding allows increased head-group proximity, enabling more efficient packing into vesicular aggregates, and thereby accounting for the significantly greater vesicle volume fractions observed at higher NaCl loadings for 10 mM OAPB/20 mM AOT (Fig. 2a). Interestingly, maintaining the same surfactant ratio (1:2, OAPB:AOT) and increasing loadings from 2.5:5 mM to 20:40 mM results in transitions from charged ellipsoids (structure factor peak at approximately $q = 0.04$ Å^{-1} gives evidence of charge) to mixtures of vesicles and worms (see SI, Fig. S5a and Table S6). This implies that micelle equilibrium geometry is dependent on ionic strength as Na^+ ions from AOT are likely contributing to charge screening effects at higher loadings where vesicles are present without added salt. With 50 mM NaCl added, even the lowest surfactant loading (2.5:5 mM, OAPB/AOT) forms a solution containing only vesicles (see SI, Fig. S5b and Table S7), reinforcing that electrolytes significantly alter the thermodynamics of self-assembly by modulating intermolecular interactions. Counter-ion concentration, degree of dissociation and additional salt have been previously noted to have significant effects on micelle aggregation and phase behaviour for systems of anionic surfactants.[47–51]

In addition to salt, the ratio of OAPB to AOT has a significant influence on the self-assembly structures formed. For 10 mM OAPB, concentrations of AOT below 10 mM result in solutions of cylindrical micelles (Fig. 2b). At 10 mM AOT and above, mixtures of vesicles and other structures are formed without salt, which conform to vesicle only solutions with 10 mM NaCl present (Fig. 2b). As OAPB has a more cylindrical molecular geometry, and AOT a more cone-shaped geometry stemming from its two, branched tail-groups, the two

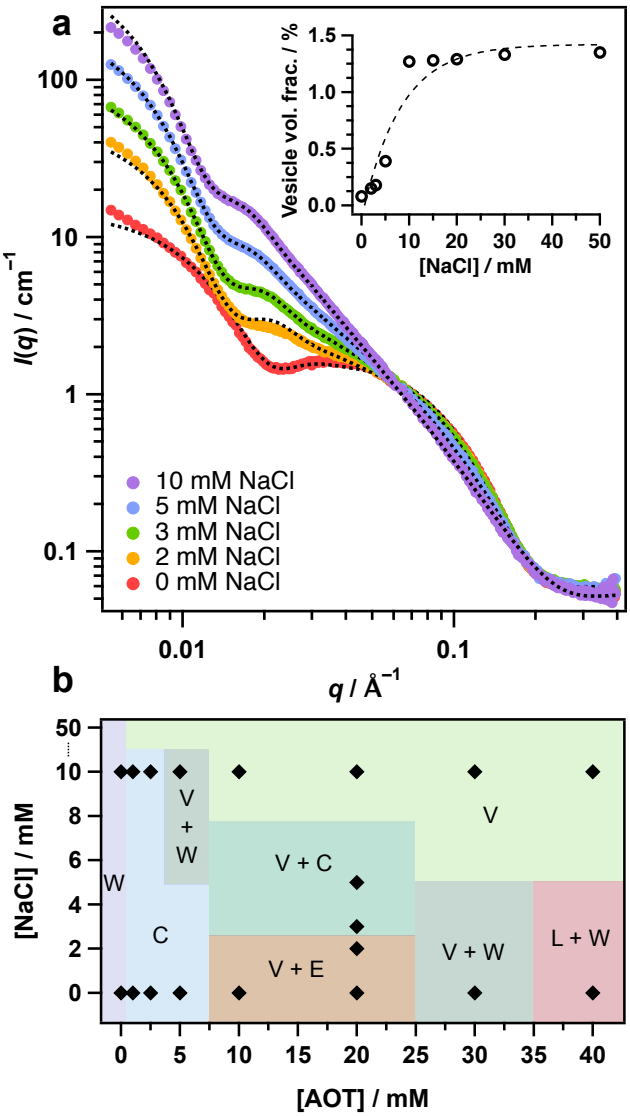

Figure 2: (a) SANS data and model fits of 10 mM OAPB and 20 mM AOT with the specified concentrations of NaCl at 25°C. The inset shows the increase in vesicle volume fraction with increasing amounts of NaCl for the same OAPB:AOT ratio. The dashed line has been added as a guide. (b) Phase diagram of self-assembled structures for samples with 10 mM OAPB and different concentrations of AOT and NaCl at 25°C. The coloured regions represent specific structures or mixtures of structures, where 'E' is ellipsoid, 'C' is cylinder, 'W' is wormlike, 'V' is vesicle and 'L' is lamellar. *Note*, phase boundaries were chosen as the halfway point between neighbouring data points in different phases, and therefore have associated uncertainty.

surfactants sterically offset one another such that the amount of each surfactant dictates the curvature of their combined packing. It is clear that higher ratios of AOT to OAPB support lower curvature interfaces, evidenced by transitions from cylinders to vesicles and then to larger radius vesicles with increasing AOT concentration. Hence, at ideal ratios, distortion between the two molecular geometries likely causes a packing arrangement in which the vesicular phase has the lowest free energy.[52,53] Scattering patterns and fitting parameters for all compositions shown in Figure 2b are given in the Supporting Information (Figs. S2 and S3, Tables 2-4).

Changes in temperature have a significant impact on the co-assembly of OAPB and AOT (Figs. 3, S6, S8 and S9). For many vesicle-forming sample compositions, heating from 25 to 37°C caused reversion of vesicular aggregates into 2-3 nm ellipsoidal micelles (see SI, Figs. S6a-c and S7 and Table S8). It is likely that increased thermal energy changes the balance of hydrophobic forces and head-group interactions, perhaps allowing greater fluidity of the tail-groups. This is well reported for lipid systems where increased temperature allows thermally induced changes in tail phase, increasing membrane fluidity.[54–56] This additional freedom could allow higher curvature structures to form. Moreover, increasing temperature acts to overcome van der Waals attractions between surfactant head-groups. This effect would ultimately alter the chemical potential of the system such that micellisation into vesicles is no longer favourable, and the aggregates must conform to higher curvature structures as a result of larger head-group areas. Previous work has also shown that heating can alter the solubility of one of the mixture components causing it to re-partition into the bulk solvent.[57] In such circumstances synergistic effects are diminished, and the system reverts towards the structures of the individual components.

When temperature is altered, salt still exerts a key influence on aggregation. A solution of 10 mM OAPB and 20 mM AOT with 3 mM NaCl forms a mixture of vesicles and

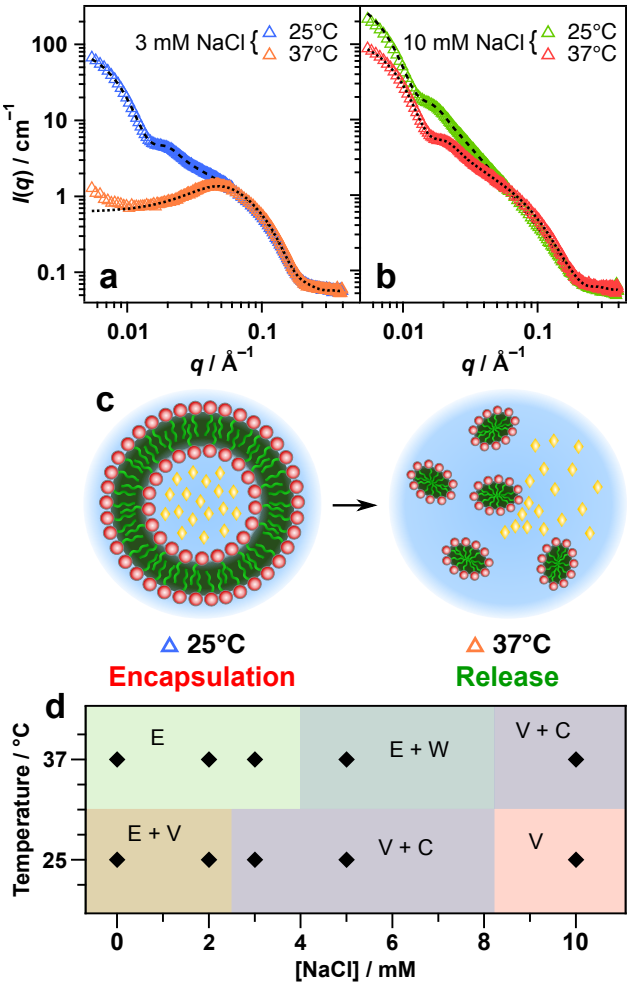

Figure 3: (a & b) SANS data and model fits of 10 mM OAPB and 20 mM AOT with 3 mM (a) and 10 mM NaCl (b) at 25 and 37°C. (c) Schematic showing the vesicle to ellipsoid structural change in (a) upon heating from 25 to 37°C, and its potential as a controlled mechanism for encapsulated compound release. The yellow diamonds represent a hypothetical water-soluble cargo. (d) Phase diagram of self-assembled structure for samples with 10 mM OAPB, 20 mM AOT and different concentrations of NaCl at 25 and 37°C. The coloured regions represent specific structures or mixtures of structures, where 'E' is ellipsoid, 'C' is cylinder, 'W' is wormlike and 'V' is vesicle .*Note*, phase boundaries were chosen as the halfway point between neighbouring data points in different phases, and therefore have associated uncertainty.

cylinders at 25°C (Fig. 3a). When heated to 37°C, the system collapses into a solution purely comprised of charged ellipsoids. Conversely, when the NaCl concentration is increased to 10 mM, heating the same surfactant composition to 37°C does not entirely disrupt vesicle formation, but causes a drop in vesicle volume fraction from 1.27% to 0.55% and coexistence of cylindrical micelles (Fig. 3b). These outcomes support the premise that formation of vesicles is dependent on molecular interactions satisfying a key curvature energy, and temperature serves to change the nature of these interactions. As salt addition in this system promotes lower curvature structures by shielding Coulombic repulsions between head-groups, the equilibrium micelle structure becomes subject to an interplay between temperature and salt concentration, as the two system variables appear to counteract each other (Fig. 3d).

This thermo-responsive behaviour could be exploited as a potential release mechanism for encapsulated materials or substances such as drugs and antibodies. In theory, the carrier compound could be encapsulated within the vesicle core as transportable cargo. Increasing temperature would then serve to trigger release of the contents at a desired time such as on entry into the body (Fig. 3c). Furthermore, because the vesicles form via noncovalent interactions, the system has the potential to be continuously reused (except in medicinal applications), as assembly and disassembly is reversible with changes in temperature. One limitation however may reside in environments where high NaCl concentrations pre-exist such as salt water or *in vivo* (154 mM NaCl in humans).[58] In such cases, further investigation and optimisation of the system will have to be performed to improve self-assembly and efficacy in saline environments. OAPB (to the best of our knowledge) has **not** been approved for *in vivo* use in any country, making the present system implausible for drug delivery. However, the combined geometries of OAPB and AOT and their resulting self-assembly structures may prove a useful reference in designing such systems that are controllable and safe to use *in vivo*. Lastly, a precise investigation of the kinetics associated with the vesicle−micelle structural transition will need to be performed before application of the system is viable.

Lastly, to further characterise vesicle self-assembly in this system and the role of salt, small-angle X-ray scattering (SAXS) measurements were performed using a series of alkali chloride salts (Fig. 4a). The salt cation was varied down group (Na→Cs) to higher electron density alkali metals, providing X-ray contrast for this consitituent. Surfactant ratio was again kept constant at 10 mM OAPB and 20 mM AOT, and the salt concentration was either 10 or 20 mM. The X-ray form factor for OAPB/AOT vesicles is similar to that obtained from SANS, in which a low q overturn is accompanied by a noticeable shoulder at approximately $q = 0.02$ Å^{-1}, corresponding to the vesicle core−shell structure. However, the SAXS patterns also exhibit a prominent peak at $q = 0.2$ Å^{-1} (Fig. 4a). This feature arises due to significant scattering contrast between surfactant head and tail regions for X-rays, and can be accounted for by modelling the vesicles with concentric layers (core−multi-shell, see SI for more detail).[26,43,59] X-ray data were hence modelled using a vesicle form factor consisting of three layers (outer head-groups, tail-groups and inner head-groups), each with a different scattering length density (SLD). This allowed accurate fitting of the high q peak, as well as an indication of surfactant and salt partitioning within the vesicle structure (Fig. 4a,b).

When changing the salt from NaCl up to CsCl, the overall intensity of the scattering becomes greater across the full q-range (Fig. 4a). This is due to stronger scattering occurring from the higher electron density cations, and provides clear evidence that a large proportion of the added electrolyte locates within the vesicle structures. For comparison, scattering from 10 mM OAPB and 20 mM AOT without salt is shown (Fig. 4a), however as SANS results from this composition revealed a mixture of different structures, this scattering pattern has not been modelled. It is clear also from the SAXS data of this sample composition that the system is not entirely vesicular.

The three shell layers each have significantly different SLDs as obtained from the fitting (see

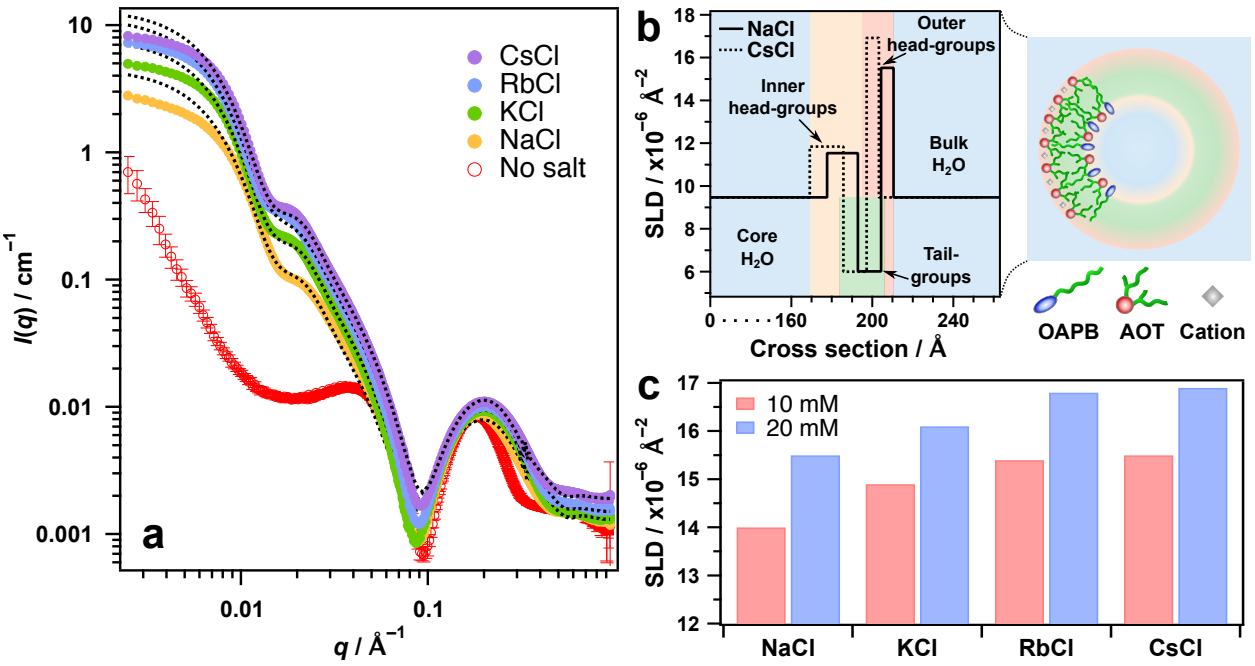

Figure 4: (a) SAXS data and model fits of 10 mM OAPB and 20 mM AOT with 10 mM of the specified salt at 25°C. (b) Scattering length density (SLD) profiles derived from modelling SAXS patterns for 10 mM OAPB and 20 mM AOT with 20 mM NaCl or CsCl using the core–multi-shell model with polydispersity in radius of the core.[34] 0 Å represents the centre of the vesicle. The schematic shows what each layer from the SLD profiles correspond to in the vesicle structure and a proposed partitioning of each surfactant type in the case of a 1:2 OAPB/AOT ratio. (c) Category plot of modelled SLDs for the outer head-group layer with each salt type at 10 and 20 mM.

SI, Fig. S10 and Table S14). Irrespective of salt identity and concentration, the interior layer unsurprisingly has the lowest SLD of around 6.0×10^{-6} Å^{-2}, corresponding to hydrophobic alkyl chains. Interestingly, a striking difference between the SLDs of the inner and outer surfactant head-group layers is observed (Fig. 4b). As with the interior layer, the SLD of the inner head-group layer (approx. 11.5×10^{-6} Å^{-2}) does not vary significantly when salt parameters are modified, suggesting that ions from added salt do not partition within this region of the vesicle structure. Conversely, the SLD of the outer head-group layer was found to not only be significantly greater than that of the inner layer, but also increased (14.0-17.0$\times10^{-6}$ Å^{-2}) when higher electron density cations and larger salt concentrations were used (Fig. 4c). We therefore conclude that added salt ions locate within this region of the vesicle, serving to increase the layer SLD. As it is only the cation of the salt that was varied, it is likely to be interacting with the anionic head-group of AOT.

We therefore posit that AOT molecules preferentially form the outer layer of the vesicles, and that the inner layer consists of a combination of OAPB and AOT molecules (see schematic, Fig. 4b). As previously stated, OAPB and AOT head-groups contain moieties of opposing charge, and hence are able to pack more densely owing to reduced electrostatic repulsive forces. AOT molecules will also pack more densely as a result of charge screening from added salt ions, however the extent to which this occurs is likely to be less than that of the co-surfactant assembly, hence why OAPB micelles have lower curvature (worms) than AOT micelles (ellipsoids). It is therefore expected that the spontaneous curvature of charge-screened AOT molecules will be lower than that of OAPB/AOT composites due to less effective screening from simple counter-ions compared to oppositely charged co-surfactants which essentially allow for negative or inverse curvature. As a result, the higher curvature monolayer naturally forms the vesicle interior, while the lower curvature monolayer locates at the exterior due to larger head-group areas.[11] The *cis*-unsaturated tail-group of OAPB likely also facilitates an inverse curvature by effecting looser packing of tail-groups,[24] further

crediting the hypothesis of an OAPB/AOT inner layer. Overall, these findings support an asymmetric distribution of the two surfactants within the vesicle structure to promote complementary spontaneous curvatures, in line with self-assembly theory for spontaneous vesicle formation.

Conclusions

Aqueous mixtures of the zwitterionic surfactant oleyl amidopropyl betaine (OAPB) and anionic surfactant Aerosol-OT (AOT) spontaneously self-assemble to form vesicles approximately 30-40 nm in diameter. The addition of salt greatly enhances vesicle formation by screening charge-based repulsions between surfactant head-groups, causing denser molecular packing and decreasing the spontaneous curvature of the micelles; salt addition also significantly increases the proportion of vesicles formed, with as little as 10 mM NaCl increasing the vesicle volume fraction by an approximate factor of 16. Mixtures of higher curvature micelles such as ellipsoids, cylinders and worms are evident from the neutron scattering form factors when no salt is added, demonstrating its importance in vesicle self assembly.

The ratio of OAPB to AOT is also a critical factor relating to aggregate geometry. AOT concentrations greater than or equal to the amount of OAPB are necessary for vesicles to form owing to a favourable packing arrangement in which excess AOT molecules enrich at the vesicle exterior. This premise is supported by small-angle X-ray scattering results, which show higher electron density counter-ions such as Rb^+ and Cs^+ also enriching at the vesicle outer layer, presumably to interact with the oppositely charged sulfonate headgroups of AOT molecules. Lower proportions of AOT also result in higher curvature micelles even in the presence of salt.

Lastly, changes in temperature exhibit marked effects on surfactant self-assembly in this

system, as a solution comprising almost entirely vesicles can be collapsed into 2-3 nm ellipsoidal micelles with no aqueous core, by heating from 25 to 37°C. This suggests potential for this system in controlled release of aqueous compounds *in vivo*, however salt concentrations of 10 mM or higher greatly inhibit this disassembly due to stronger intermolecular binding. These findings provide new, fundamental insights into tailoring surfactant mixtures for spontaneous vesicle self-assembly based on molecular geometry and physicochemical properties. Such systems exploit common, inexpensive and low toxicity[14,15,60,61] surfactants, and could be used as destructible and reformable delivery vessels for controlled compound release in aqueous environments.

Acknowledgements

We would like to acknowledge the Australian Centre for Neutron Scattering and the National Deuteration Facility, Australian Nuclear Science and Technology Organisation, for beamtime and provision of materials. The National Deuteration Facility is partly supported by the National Collaborative Research Infrastructure Strategy – an initiative of the Australian Government. We also thank the Australian Institute of Nuclear Science and Engineering and the Monash Centre for Atomically Thin Materials for additional funding to T.M.M. This work was supported in part by the grant of an Australian Research Council Future Fellowship (FT160100191) to R.F.T. and a Discovery Early Career Research Award (DE190100531) to A.J.C.

Supporting Information

File contains:

- Additional SANS and SAXS patterns
- Tables of fitting parameters used in modeling scattering patterns
- Details of models and modeling procedures

References

(1) Israelachvili, J. N.; Mitchell, D. J.; Ninham, B. W. Theory of self-assembly of hydrocarbon amphiphiles into micelles and bilayers. *J. Chem. Soc. Faraday Trans.* **1976**, *72*, 1525–1568.

(2) Israelachvili, J. N.; Mitchell, D. J.; Ninham, B. W. Theory of self-assembly of lipid bilayers and vesicles. *Biochim. Biophys. Acta* **1977**, *470*, 185–201.

(3) Bucher, P.; Fischer, A.; Luisi, P. L.; Oberholzer, T.; Walde, P. Giant vesicles as biochemical compartments: the use of microinjection techniques. *Langmuir* **1998**, *14*, 2712–2721.

(4) Stamou, D.; Duschl, C.; Delamarche, E.; Vogel, H. Self-assembled microarrays of attoliter molecular vessels. *Angew. Chem. Int. Ed.* **2003**, *42*, 5580–5583.

(5) Bolinger, P.-Y.; Stamou, D.; Vogel, H. Integrated nanoreactor systems: triggering the release and mixing of compounds inside single vesicles. *J. Am. Chem. Soc.* **2004**, *126*, 8594–8595.

(6) Vader, P.; Mol, E. A.; Pasterkamp, G.; Schiffelers, R. M. Extracellular vesicles for drug delivery. *Adv. Drug Deliv. Rev.* **2016**, *106*, 148–156.

(7) Sinico, C.; Fadda, A. M. Vesicular carriers for dermal drug delivery. *Expert Opin. Drug. Deliv.* **2009**, *6*, 813–825.

(8) Israelachvili, J. N. *Intermolecular and Surface Forces*; Academic Press: San Diego, 1991.

(9) Kaler, E. W.; Murthy, A. K.; Rodriguez, B. E.; Zasadzinski, J. A. N. Spontaneous Vesicle Formation in Aqueous Mixtures of Single-Tailed Surfactants. *Science* **1989**, *245*, 1371–1374.

(10) Hargreaves, W. R.; Deamer, D. W. Liposomes from ionic, single-chain amphiphiles. *Biochemistry* **1978**, *17*, 3759–3768, PMID: 698196.

(11) Safran, S. A.; Pincus, P.; Andelman, D. Theory of Spontaneous Vesicle Formation in Surfactant Mixtures. *Science* **1990**, *248*, 354–356.

(12) Kaler, E. W.; Herrington, K. L.; Murthy, A. K.; Zasadzinski, J. A. Phase behavior and structures of mixtures of anionic and cationic surfactants. *J. Phys. Chem.* **1992**, *96*, 6698–6707.

(13) Jung, H.; Coldren, B.; Zasadzinski, J.; Iampietro, D.; Kaler, E. The origins of stability of spontaneous vesicles. *Proc. Natl. Acad. Sci. U.S.A.* **2001**, *98*, 1353–1357.

(14) Burnett, C. L.; Bergfeld, W. F.; Belsito, D. V.; Hill, R. A.; Klaassen, C. D.; Liebler, D.; Marks Jr, J. G.; Shank, R. C.; Slaga, T. J.; Snyder, P. W.; Anderson, A. F. Final report of the Cosmetic Ingredient Review Expert Panel on the safety assessment of cocamidopropyl betaine (CAPB). *Int. J. Toxicol.* **2012**, *31*, 77S–111S.

(15) Gheorghe, S.; Lucaciu, I.; Paun, I.; Stoica, C.; Stanescu, E. Ecotoxicological behavior of some cationic and amphoteric surfactants (biodegradation, toxicity and risk assessment). *Biodegradation - Life of Science* **2013**, 83–114.

(16) Hunter, J. E.; Fowler, J. F. Safety to human skin of cocamidopropyl betaine: a mild surfactant for personal-care products. *J. Surfactants Deterg.* **1998**, *1*, 235–239.

(17) Leidreiter, H.; Gruning, B.; Kaseborn, D. Amphoteric surfactants: processing, product composition and properties. *Int. J. Cosmet. Sci.* **1997**, *19*, 239–253.

(18) Kumar, R.; Kalur, G. C.; Ziserman, L.; Danino, D.; Raghavan, S. R. Wormlike Micelles of a C22-Tailed Zwitterionic Betaine Surfactant: From Viscoelastic Solutions to Elastic Gels. *Langmuir* **2007**, *23*, 12849–12856.

(19) Chu, Z.; Feng, Y.; Su, X.; Han, Y. Wormlike micelles and solution properties of a C22-tailed amidosulfobetaine surfactant. *Langmuir* **2010**, *26*, 7783–7791.

(20) Spenley, N. A.; Cates, M. E.; McLeish, T. C. B. Nonlinear rheology of wormlike micelles. *Phys. Rev. Lett.* **1993**, *71*, 939–942.

(21) Chu, Z.; Dreiss, C. A.; Feng, Y. Smart wormlike micelles. *Chem. Soc. Rev.* **2013**, *42*, 7174–7203.

(22) Dreiss, C. A. Wormlike micelles: where do we stand? Recent developments, linear rheology and scattering techniques. *Soft Matter* **2007**, *3*, 956–970.

(23) McCoy, T. M.; Valiakhmetova, A.; Pottage, M. J.; Garvey, C. J.; de Campo, L.; Rehm, C.; Kuryashov, D. A.; Tabor, R. F. Structural Evolution of Wormlike Micellar Fluids Formed by Erucyl Amidopropyl Betaine with Oil, Salts, and Surfactants. *Langmuir* **2016**, *32*, 12423–12433.

(24) Kelleppan, V. T.; Moore, J. E.; McCoy, T. M.; Sokolova, A. V.; de Campo, L.; Wilkinson, B. L.; Tabor, R. F. Self-Assembly of Long-Chain Betaine Surfactants: Effect of Tailgroup Structure on Wormlike Micelle Formation. *Langmuir* **2017**, *34*, 970–977.

(25) Gilbert, E. P.; Schulz, J. C.; Noakes, T. J. Quokka - the small-angle neutron scattering instrument at OPAL. *Physica B* **2006**, *385-386*, 1180–1182.

(26) Kline, S. R. Reduction and analysis of SANS and USANS data using IGOR Pro. *J. Appl. Crystallogr.* **2006**, *39*, 895–900.

(27) Kirby, N. M.; Mudie, S. T.; Hawley, A. M.; Cookson, D. J.; Mertens, H. D.; Cowieson, N.; Samardzic-Boban, V. A low-background-intensity focusing small-angle X-ray scattering undulator beamline. *J. Appl. Crystallogr.* **2013**, *46*, 1670–1680.

(28) Pedersen, J. S.; Schurtenberger, P. Scattering Functions of Semiflexible Polymers with and without Excluded Volume Effects. *Macromolecules* **1996**, *29*, 7602–7612.

(29) Chen, W.-R.; Butler, P. D.; Magid, L. J. Incorporating intermicellar interactions in the fitting of SANS data from cationic wormlike micelles. *Langmuir* **2006**, *22*, 6539–6548.

(30) Kuryashov, D.; Philippova, O.; Molchanov, V.; Bashkirtseva, N. Y.; Diyarov, I. Temperature effect on the viscoelastic properties of solutions of cylindrical mixed micelles of zwitterionic and anionic surfactants. *Colloid J.* **2010**, *72*, 230–235.

(31) McCoy, T. M.; King, J. P.; Moore, J. E.; Kelleppan, V. T.; Sokolova, A. V.; de Campo, L.; Manohar, M.; Darwish, T. A.; Tabor, R. F. The effects of small molecule organic additives on the self-assembly and rheology of betaine wormlike micellar fluids. *J. Colloid Interface Sci.* **2019**, *534*, 518 – 532.

(32) Candau, S.; Hirsch, E.; Zana, R.; Adam, M. Network properties of semidilute aqueous KBr solutions of cetyltrimethylammonium bromide. *J. Colloid Interface Sci.* **1988**, *122*, 430–440.

(33) Magid, L. J.; Li, Z.; Butler, P. D. Flexibility of Elongated Sodium Dodecyl Sulfate Micelles in Aqueous Sodium Chloride: A Small-Angle Neutron Scattering Study. *Langmuir* **2000**, *16*, 10028–10036.

(34) Feigin, L.; Svergun, D. I.; Taylor, G. W. *Structure analysis by small-angle X-ray and neutron scattering*; Springer, 1987; pp 25–55.

(35) Hayter, J. B.; Penfold, J. An analytic structure factor for macroion solutions. *Mol. Phys.* **1981**, *42*, 109–118.

(36) Hayter, J. B.; Penfold, J. Self-consistent Structural and Dynamic Study of Concentrated Micelle Solutions. *J. Chem. Soc., Faraday Trans. I* **1981**, *77*, 1851–1863.

(37) Hansen, J.-P.; Hayter, J. B. A rescaled MSA structure factor for dilute charged colloidal dispersions. *Molecular Physics* **1982**, *46*, 651–656.

(38) Hayter, J. B.; Penfold, J. Determination of Micelle Structure and Charge by Small-Angle Neutron Scattering. *Colloid Polym. Sci.* **1983**, *261*, 1022–1030.

(39) Wu, C.; Chan, D. Y.; Tabor, R. F. A simple and accurate method for calculation of the structure factor of interacting charged spheres. *J. Colloid Interface Sci.* **2014**, *426*, 80–82.

(40) Nave, S.; Eastoe, J.; Penfold, J. What is so special about Aerosol-OT? 1. Aqueous systems. *Langmuir* **2000**, *16*, 8733–8740.

(41) Nave, S.; Eastoe, J.; Heenan, R. K.; Steytler, D.; Grillo, I. What is so special about aerosol-OT? 2. Microemulsion systems. *Langmuir* **2000**, *16*, 8741–8748.

(42) McCoy, T. M.; de Campo, L.; Sokolova, A. V.; Grillo, I.; Izgorodina, E. I.; Tabor, R. F. Bulk properties of aqueous graphene oxide and reduced graphene oxide with surfactants and polymers: adsorption and stability. *Phys. Chem. Chem. Phys.* **2018**, *20*, 16801–16816.

(43) Guinier, A.; Fournet, G.; Walker, C. *Small angle scattering of X-rays*; J. Wiley & Sons, New York, 1955.

(44) Tanford, C. Micelle shape and size. *J. Phys. Chem.* **1972**, *76*, 3020–3024.

(45) Andreozzi, P.; Funari, S. S.; La Mesa, C.; Mariani, P.; Ortore, M. G.; Sinibaldi, R.; Spinozzi, F. Multi-to unilamellar transitions in catanionic vesicles. *J. Phys. Chem. B* **2010**, *114*, 8056–8060.

(46) Söderman, O.; Herrington, K. L.; Kaler, E. W.; Miller, D. D. Transition from micelles to vesicles in aqueous mixtures of anionic and cationic surfactants. *Langmuir* **1997**, *13*, 5531–5538.

(47) Bales, B. L.; Zana, R. Cloud point of aqueous solutions of tetrabutylammonium dodecyl

sulfate is a function of the concentration of counterions in the aqueous phase. *Langmuir* **2004**, *20*, 1579–1581.

(48) Ranganathan, R.; Tran, L.; Bales, B. L. Surfactant-and salt-induced growth of normal sodium alkyl sulfate micelles well above their critical micelle concentrations. *J. Phys. Chem. B* **2000**, *104*, 2260–2264.

(49) Griffiths, P. C.; Paul, A.; Heenan, R.; Penfold, J.; Ranganathan, R.; Bales, B. L. Role of counterion concentration in determining micelle aggregation: Evaluation of the combination of constraints from small-angle neutron scattering, electron paramagnetic resonance, and time-resolved fluorescence quenching. *J. Phys. Chem. B* **2004**, *108*, 3810–3816.

(50) Barchini, R.; Pottel, R. Counterion contribution to the dielectric spectrum of aqueous solutions of ionic surfactant micelles. *J. Phys. Chem.* **1994**, *98*, 7899–7905.

(51) Lebedeva, N. V.; Shahine, A.; Bales, B. L. Aggregation number-based degrees of counterion dissociation in sodium n-alkyl sulfate micelles. *J. Phys. Chem. B* **2005**, *109*, 19806–19816.

(52) Weiss, T. M.; Narayanan, T.; Wolf, C.; Gradzielski, M.; Panine, P.; Finet, S.; Helsby, W. I. Dynamics of the Self-Assembly of Unilamellar Vesicles. *Phys. Rev. Lett.* **2005**, *94*, 038303.

(53) Ghosh, S.; Khatua, D.; Dey, J. Interaction between zwitterionic and anionic surfactants: spontaneous formation of zwitanionic vesicles. *Langmuir* **2011**, *27*, 5184–5192.

(54) Amatruda, J. M.; Finch, E. D. Modulation of hexose uptake and insulin action by cell membrane fluidity. The effects of temperature on membrane fluidity, insulin action, and insulin binding. *J. Biol. Chem.* **1979**, *254*, 2619–2625.

(55) Murata, N.; Los, D. A. Membrane fluidity and temperature perception. *Plant Physiol.* **1997**, *115*, 875.

(56) Mansilla, M. C.; Cybulski, L. E.; Albanesi, D.; de Mendoza, D. Control of membrane lipid fluidity by molecular thermosensors. *J. Bacteriol.* **2004**, *186*, 6681–6688.

(57) Davies, T. S.; Ketner, A. M.; Raghavan, S. R. Self-Assembly of Surfactant Vesicles that Transform into Viscoelastic Wormlike Micelles upon Heating. *J. Am. Chem. Soc.* **2006**, *128*, 6669–6675.

(58) Wilcox, C. S. Regulation of renal blood flow by plasma chloride. *J. Clin. Investig.* **1983**, *71*, 726–735.

(59) Clulow, A. J.; Parrow, A.; Hawley, A.; Khan, J.; Pham, A. C.; Larsson, P.; Bergström, C. A.; Boyd, B. J. Characterization of Solubilizing Nanoaggregates Present in Different Versions of Simulated Intestinal Fluid. *J. Phys. Chem. B* **2017**, *121*, 10869–10881.

(60) Changez, M.; Varshney, M. Aerosol-OT microemulsions as transdermal carriers of tetracaine hydrochloride. *Drug Dev. Ind. Pharm.* **2000**, *26*, 507–512.

(61) Wilson, J. L.; Dickinson, D. G. Use of dioctyl sodium sulfosuccinate (aerosol OT) for severe constipation. *JAMA* **1955**, *158*, 261–263.

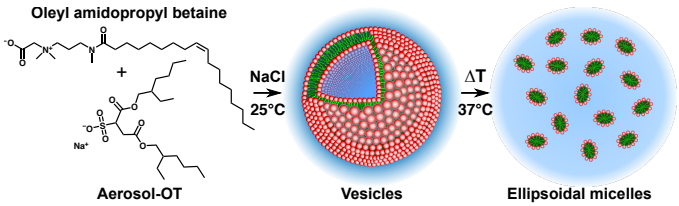

For Table of Contents Use only

Spontaneous self-assembly of vesicles using a zwitterionic and anionic surfactant as thermo-responsive carriers

Thomas M. McCoy, Joshua B. Marlow, Alexander J. Armstrong, Andrew J. Clulow, Christopher J. Garvey, Madhura Manohar, Tamim A. Darwish, Ben J. Boyd, Alexander F. Routh and Rico F. Tabor